USING NUMERICAL MODELLING TO ANALYZE BEACH PROFILES RESPONSE TO EXTREME STORMS ALONG THE DANUBE DELTA COAST, ROMANIA

Irina DINU[1], Manuel GARCÍA-LEÓN[2], Vicente GRÀCIA[2], Agustín SÁNCHEZ-ARCILLA[2], Adrian STĂNICĂ[1]

[1]National Institute of Marine Geology and Geo-Ecology (GeoEcoMar), 23-25 Dimitrie Onciul St., 024053 Bucharest, Romania
e-mail: irinadinu@geoecomar.ro, astanica@geoecomar.ro
[2]Maritime Engineering Laboratory, Polytechnic University of Barcelona – Barcelona Tech, 1-3, Jordi Girona, 08034, Barcelona, Spain
e-mail: manuel.garcia-leon@upc.edu, vicente.gracia@upc.edu, agustin.arcilla@upc.edu

Abstract. In recent decades, human interventions along the Danube River have played a major influence on the reduction of sediment supply along the Danube Delta coast, which is nowadays affected by erosion on its widest part. The Danube Delta coast is part of the Danube Delta Biosphere Reserve, thus being designated to preserve its typical natural habitats. Therefore, Working-with-Nature concepts can be included in order to establish a sustainable maintenance plan. A method to assess the impact of storms on beach profiles along the Danube Delta is proposed in this paper. To this purpose two beach profiles located in the zone of the Sf. Gheorghe mouth have been chosen. The results of a Wave Climate Analysis have been used in order to reproduce extreme storms, as well as the model XBeach in 1D approach, to simulate their effect on the chosen profiles. The proposed analysis represents a quick and effective way to estimate the damage of extreme storms on individual beach profiles.

Key words: climate change, wave height, mean water level, sand volume change, assymptotic behaviour, resilience

1. INTRODUCTION

The Danube Delta Biosphere Reserve is both a UNESCO and a RAMSAR site.The strategic objective for this zone is to ensure its sustainable development, by preserving the typical natural habitats with significant biodiversity and also the traditional way of life for the local communities, while taking care to improve their living standards.

Climate change is expected to lead to the increase of the frequency of storms and of the mean sea level in Europe (Kovats *et al.*, 2014). This will have a direct impact on low-lying coasts, such as the Danube Delta coast. Beach erosion is essential in coastal zone management (Lisi *et al.*, 2013). Therefore, quantifying the effects of severe storms on beaches is a challenging objective.

Due to its pristine environment, it is recommended to have a Working-with-Nature strategy for the coastal management (HALCROW UK *et al.*, 2011-2012). In order to do that, it is important to understand the behaviour of the beach to storm impact, under present climate change scenarios.

The Danube Delta coast has a total length of about 240 km, extending both in Ukraine and Romania. The Romanian part of the Danube Delta coast is a stretch of 160 km of low-lying natural beaches generally consisting of fine sands brought by the Danube River and redistributed by waves and currents. This area's morphology, sedimentology and recent dynamics have been extensively studied and described by a series of publications (Panin, 1996, 1998, 1999, 2003; Giosan *et al.*, 1999; Ungureanu and Stănică, 2000; Bhattacharya and Giosan, 2003; Stănică *et al.*, 2007, 2011; Vespremeanu-Stroe *et al.*, 2007; Stănică and Panin, 2009; Dan *et al.*, 2009; Dan, 2013).

The Danube River discharges into the Black Sea through three distributaries that are, from North to South: Kilia, which transports approximately 51.6% of the water discharge; Sulina, the major waterway, with 19.9% and Sfântu Gheorghe, 24.4%, the rest of the water being discharged through Ra-

zelm-Sinoe lagoon system (Bondar and Panin, 2001). The distribution of the sediment discharge is slightly different: Kilia – 53.3%, Sulina – 15.8%, Sfântu Gheorghe – 21.9%, while the rest is being deposited in the Danube Delta (Bondar and Panin, 2001).

Water circulation in the Romanian coastal zone has been simulated with a 3D finite element hydrodynamic model by Bajo *et al.*, 2014. The model results have shown that the complex dynamics generated along the Romanian coast is due to the interaction of various factors, such as the wind, the Danube's freshwater discharge, the sea level, but also the temperature and salinity distributions. These changes are even higher during storm events.

In their analysis of the storminess in the Northwestern part of the Black Sea, based on hindcast data series for the time interval between 1948 and 2010, Valchev *et al.* 2012, state that the most intense and frequent winds directed onshore, that trigger the severest storms, are those from NE, E and SE. Wave conditions were modelled using a coupled system of third generation spectral wave models. Identification of storms was based primarily on wind data. Only winds within directional segment 0 – 180°N were considered, as they are directed shoreward. These authors provide a description for the typical storm in the Northwestern part of the Black Sea, that includes the whole Romanian coast. According to this, it is estimated that storm duration varies between 56 hours and 151 hours and the average duration is 95 hours. Extreme storms have a quite short growth phase, the phase of the full development is more substantial while the decay time is the longest. The average duration of the phase of full development is 61 h and is longer than both the first and the second phases put together, which last 18 and 41 h, respectively (Valchev *et al.*, 2012).

The wind wave fields in the Black Sea have been studied by Arkhipkin *et al.*, 2014, using the SWAN model (Booij *et al.*, 1999). These authors state that the Northeastern and the Southwestern parts of the Black Sea are the ones with the highest significant wave heights and the most intense storminess. The wave-current interactions at the Danube's mouths have been studied by Rusu, 2009; 2010, also using the SWAN model (Booij *et al.*, 1999). This author states that the relatively strong currents induced there by the outflow from the Danube modifies considerably both the wave magnitude and direction, affecting also the coastal navigation and the sediment transport patterns. The SWAN model has also been used by Dan, 2013, to analyze the wave climate along the Danube Delta coast. In this study, three main wave directions have been identified: the Northern directions (N to ENE), that produce the largest average wave heights; the Eastern directions (E to SE), with the lowest average wave heights; and the Southern directions (SSE to WSW), that produce medium average wave heights.

Sánchez-Arcilla *et al.*, 2016 show that the SLR at the Eastern Mediterranean coast (strongly connected with the Black Sea) may reach more than 60 cm at the end of the 21st century.

The aim of this paper is to assess the damage that may occur on the Danube Delta coast in case of extreme storms, under present climate change conditions. For this study, we have selected the area comprising the mouth of the Sf. Gheorghe distributary of the Danube, as measurements on a couple of beach profiles have been performed in several field campaigns, in recent years (Vespremeanu-Stroe and Preoteasa, 2007; Tătui *et al.*, 2016).

A way to determine such impact is with numerical modelling (Gràcia *et al.*, 2013; Lesser *et al.*, 2004; Sánchez-Arcilla *et al.*, 2014). In these articles, a hydromorphodynamic model (Roelvink *et al.*, 2009), once calibrated, has been used to assess the post-storm evolution of the morphodynamic impact of the Danube coast.

The paper is structured as follows: the Methodology section includes the datasets (beach profiles and wave climate) that have been used and the description of the simulations and metrics; Results for both beach profiles are presented; followed by the Discussion and Conclusions.

2. METHODOLOGY

Beach profiles

Two cross-shore beach profiles have been chosen, NR48 and Buival, located North of the Sf. Gheorghe distributary of the Danube (Fig. 1). Both beach profiles have dunes, that could be destroyed in case of extreme storms.

The topographic surveys were undertaken using a Leica VIVA GS12 RTK DGPS (horizontal accuracy of 5 mm + 0.5 ppm and vertical accuracy of 10 mm + 0.5 ppm) from back of dunes to 1 m depth. The underwater part of the profiles was surveyed using a Valeport Midas Surveyer single-beam echo-sounder (accuracy ±0.01m). All data were registered in the Romanian geodetic system (Stereo 70), which eased the joint of the topographic data with the bathymetric ones for the same profile.

Tătui *et al.*, 2016 state that the zone where the Buival profile is located is advancing, the NR48 profile is located in a stable zone, while the northward shoreline is retreating. The dominant longshore direction in front of the Danube Delta is from North to South (Giosan *et al.*, 1999; Panin and Jipa, 2002; Stănică *et al.*, 2007). Yankovsky *et al.*, 2004 analyzed the influence of the Danube buoyant flow on the Northwestern part of the Black Sea. The Sf. Gheorghe distributary takes over more than 20% of the total Danube discharge (Bondar and Panin, 2001), therefore it certainly influences the water and sediment dynamics in the study area. Both profiles show low elevation at the emerged part and a dissipative, gentle beach slope. The sediment size in the study area is around 200 microns, based on the multi-annual sediment analyses (HALCROW UK et al, 2011-2012).

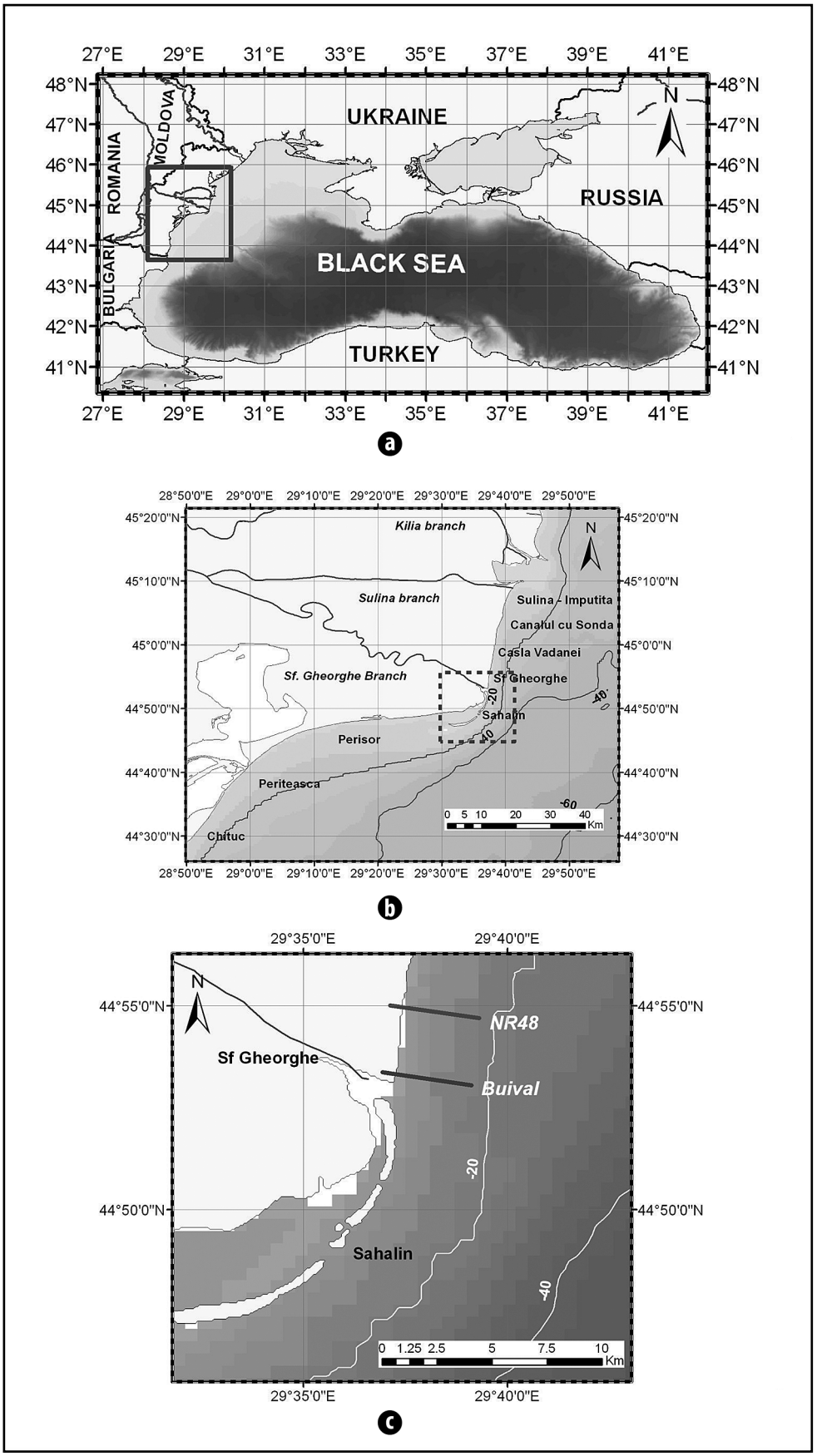

Fig. 1. a) Black Sea map; **b)** Danube Delta map; **c)** Location of the NR48 and Buival profiles on the Danube delta coast

Hydrodynamic forcings

Moderate storms, that occurred in between February 10 and 27, 2016, have beeen used to fit the XBeach model in 1D approach. The waves available for this time interval have been provided by the GeoEcoMar wave gauge, located on the Southern part of the Romanian coast. The sea level has been measured at the Sulina coastal station, owned by GeoEcoMar. The maximum wave height is 2.51 m and the associated wave period is 7.04 s. Most of the waves, about 65%, are from the Southeastern sector. The mean sea level is around 0, with a minimum of -14 cm and a maximum of 20 cm. Figure 2 shows the wave heights, wave periods, wave directions and the sea level between February 10 and 27, 2016.

Once the model has been calibrated, the storms applied are available from a Wave Climate Analysis, carried out by Johnson, 2011 within the Master Plan for Reduction of Coastal Erosion on the Black Sea Coast (2011-2012). The Wave Climate Analysis provided maximum wave heights and associated wave periods for storms from various sectors. The ones from SE, S and E have been selected, as they are the ones that

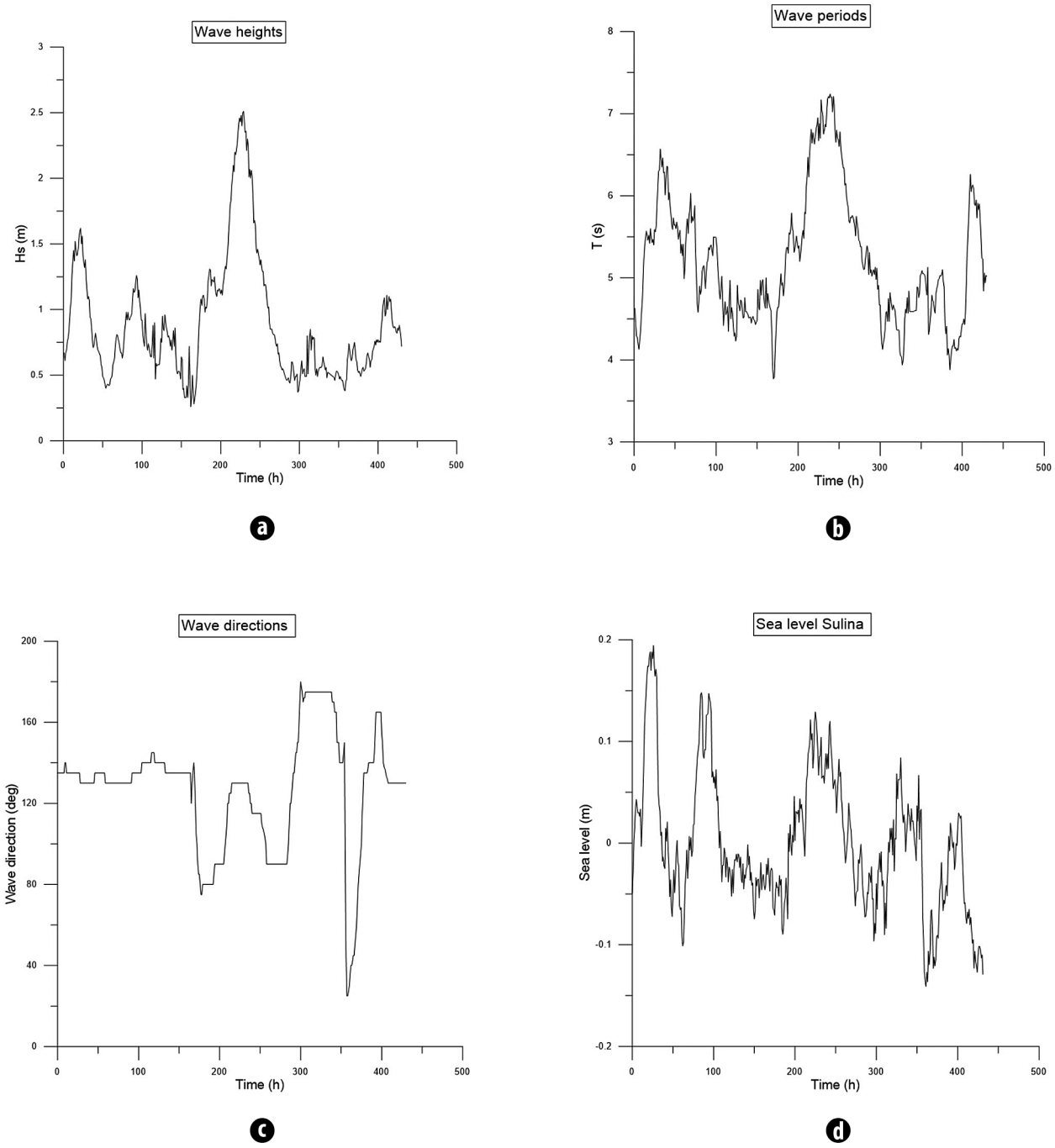

Fig. 2. Forcings used in the XBeach simulations, for the period February 10 to 27, 2016 – **a)** wave heights; **b)** wave periods; **c)** wave directions; **d)** sea level

cause damage to the beaches on the Danube Delta coast. According to these results, the extreme storms from S and E have higher maximum wave heights and associated wave periods than the ones from SE (Johnson, 2011).

In order to reproduce such storms, we took into account the above-mentioned Wave Climate Analysis results, as well as the storm description for the Western Black Sea, available in the work of Valchev *et al*. 2012. The authors estimated that the average duration of extreme storms is 95 hours and that they have a short growth phase, a more substantial full development phase and a long decay time.

The waves from SE derived from the Wave Climate Analysis (Johnson, 2011) have lower wave heights and wave periods than the ones from S and E (Table 1).

There are no studies concerning how the Sea Level will change for the Black Sea. In order to study the impact of Sea Level Rise (SLR), we have performed several simulations, with the Mean Water Level progressively increased by 0.2 m. Thus, the Mean Water Level has the following values: 0, 0.2, 0.4, 0.6, 0.8, and 1 m.

The range of MWL values can be considered reasonable because: (i) In recent studies, an approximation of a 0.88 m SLR has been used at the NW Mediterranean Sea for the RCP 8.5 scenario (Sierra *et al.*, 2016) at the end of the 21st century. (ii) Altimeter information shows that the SLR at the Eastern Mediterranean and the Black Sea is correlated. (iii) Jevrejeva *et al.*, 2014 have analysed the upper limits of the different components of the SLR projections and the global SLR values can reach up to 1.8 m for the same scenario, although the probability is low. These values are also in agreement with the available projected global mean sea level for the 2081 – 2100 interval (Kovats *et al.*, 2014).

The assumption of 0.88 m SLR within the 21st century comes justified by the estimations of Jevrejeva *et al.*, 2014 at a global scale. Despite it is true that, in the Mediterranean, SLR it is considered around 60 cm as a mean value in the IPCC WG1, 2013 report, it has to be taken into account that the upper part of the confidence interval (95%) is around 90 cm. Hence, this approximation follows a safety side. There is so much uncertainty on the Sea Level Rise that some authors recommend taking the upper values of the confidence intervals in Impact-Vulnerability Studies (see Hinkel *et al.*, 2015). The SLR projections for different RCPs can also be found in Sánchez-Arcilla *et al.*, 2016. In the latter reference it can be observed that the upper values match considerably with the ones in Sierra, 2016.

Figure 3 shows the workflow. The simulations have been performed for each Return Period taken into account, for 6 values of the Mean Water Level, and for the 3 wave directions which would have an impact on the beach. A total number of 72 simulations have been performed for each profile.

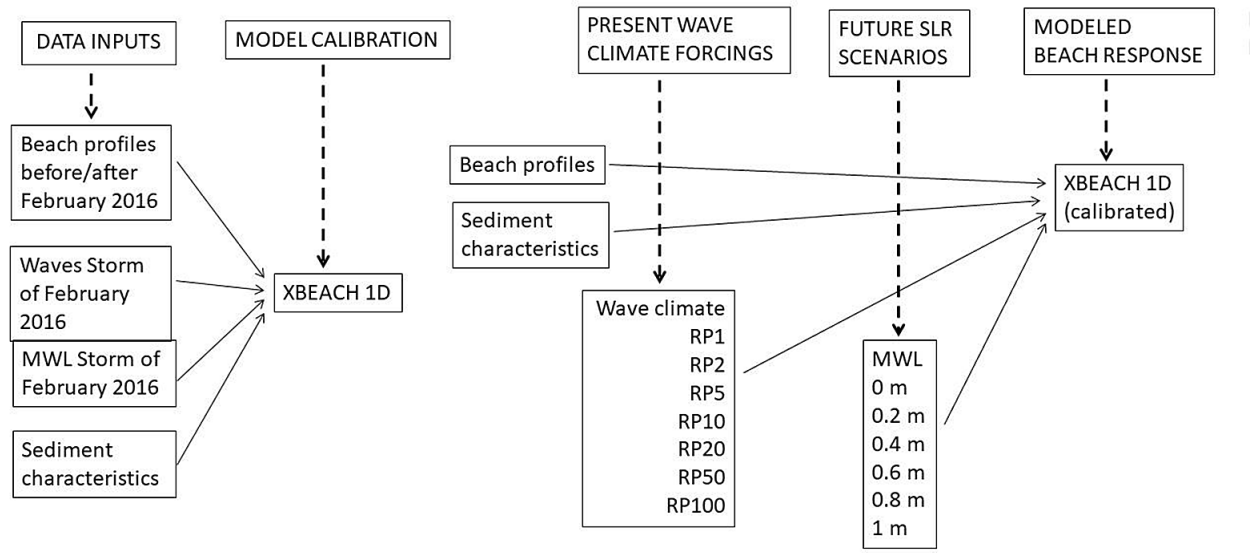

Fig. 3. Methodology flow chart

Table 1. Maximum Wave Height *Hs* and associated Wave Period *T* for the extreme storms derived from the Wave Climate Analysis – from Johnson, 2011

	SE storms		S storms		E storms	
***RP* (years)**	H_s **(m)**	***T* (s)**	H_s **(m)**	***T* (s)**	H_s **(m)**	***T* (s)**
1	1.4	6.02	2.4	7.01	1.85	7.03
2	2.05	7.01	3.4	8.11	2.9	8.16
5	2.6	7.71	4	8.68	3.85	8.96
10	3	8.16	4.3	8.95	4.45	9.39

Numerical modelling

The open-source model XBeach (Roelvink *et al.*, 2009) has been used to model the nearshore response to storms for the analyzed profiles located on the Danube Delta coast. The XBeach model is able to simulate dune erosion, overwashing and breaching. The processes are modelled in four different regimes of impact on barrier islands by hurricanes, which are, according to Sallenger, 2000: the 1) swash regime, 2) collision regime, 3) overwash regime and 4) inundation regime.

Both short wave action and long wave action are taken into account. In our work, XBeach has been used in 1D approach to simulate the effect of storms on the Danube Delta coast. Hence, the results infer the behaviour of the cross-shore fluxes.

The sand volume change following a storm has been determined as the area between the emerged part of the pre-storm and the post-storm profiles, as percentage of the initial emerged profile.

The runup has been calculated using the Stockdon equation (Stockdon *et al.*, 2006):

$$runup = 1.1\times\left(0.35\beta_f\left(H_0L_0\right)^{\frac{1}{2}} + \frac{\left[H_0L_0\left(0.563\beta_f^2+0.004\right)\right]^{\frac{1}{2}}}{2}\right)$$

where: $L_0 = \frac{gT_p^2}{2\pi}$

In the above relations, β_f is the foreshore slope, H_0 is the deep water wave height, L_0 is the deep water wave length, T_p is the peak period, and g is the gravity acceleration.

The value for H_0 is 0.82 m, taken from altimeter data in an offshore point near the Danube delta (https://www.aviso.altimetry.fr). The value for T_p is 4.3 s, estimated based on the available data in Sf. Gheorghe area.

In our analysis we use a Resilience Ratio (*RR*), defined as:

$$RR = \frac{runup + SLR}{post\text{-}storm\ elevation}$$

where SLR is the Sea Level Rise (in meters) and the post-storm elevation is defined as following: if there is a dune, it is the mean elevation of the emerged post-storm profile from the toe of the dune to the shoreline; if there is no dune, it is the average elevation of the post-storm emerged profile.

This metric provides a view on how the coast will be prepared for the next storm. *RR* value below 1 means that the joint action of waves and sea level for a given storm would not surpass the post-storm elevation. Hence, the protection system which, in our case, is represented by the dune, will not collapse. There may be collision and overwash regime, but not inundation (Sallenger, 2000). However, once the RR values surpass the unity, most surely, inundation regime will occur. This index aims to reflect that the initial conditions of the beach profile will be perturbed once a storm event has happened. Then, from a management point of view it is important to know the protection capacity of the beach, once the storm has happened. *RR* can prompt action, because it shows the weak spots, supporting decision making on what parts of a coastal strech require intervention once a storm has happened.

Other indexes have been used in previous works (see Chiaia *et al.*, 1992) explaining sand volume displacement along the profiles and bar growth and displacement. The simulations performed have shown more sand erosion at the emerged part than in the submerged part.

The dominance of emerged sand dynamics for this kind of short-term scale was the reason that we used the *RR* metric. It could be possible to compute bar growth and displacements, but the results will not be as interesting as the emerged beach ones, that are the ones that have been highlighted in the paper. Note that the dominance of emerged sand dynamics during storms does not need to happen at all case studies; but as it can be seen in the results, for this particular time-scale and study area, the abovementioned behaviour happens.

Nonetheless, we consider that at mid-scale and long-term scale, bar dynamics (growth and displacement) play a fundamental role in the hydrodynamics and the proposed indexes in Chiaia *et al.* (1992) should be used for sure.

The calibrated model has been used for assessing a Tipping Point due to climate change. In this case, erosion of the emerged part, due to extreme events, has been used as an environmental indicator.

In order to assess a Tipping Point, specific analysis has been carried out on each profile. The purpose of this analysis has been to see if an assymptotic value for the eroded sand volume is reached, given a set of incremental drivers. This means that the eroded sand volume tends to reach a maximum value with respect to the SLR and/or to the intensity of the storm. Starting from a certain Mean Water Level or from a certain Return Period of the storm, the eroded sand volume is not expected to change significantly. Such an analysis could help in estimating the SLR or the storm intensity starting with which severe damage could occur to the beach profile, thus being useful in assessing appropriate coastal protection measures.

Assymptotic behaviour is the state in which the protection system has collapsed. It does not matter that we add more intensity to the drivers, the response will be the same. It will be analogous to a saturated system. The assymptota shows that there is no further growth. Assymptotic behaviour bounds the upper limit of the consequences/impacts. It is 100% damage; and this 100% usually is hard to obtain for most of the natural disaster processes. Hence, it is a confirmatory analysis that is really interesting to have. Otherwise, it can be hard to backtrack what is the damage level given a set of drivers.

The results of the simulations with extreme storms are analyzed in order to estimate the damage that may occur to the beach profiles and to establish Tipping Points.

3. RESULTS

The impact assesment has two steps: calibration of the model and its validation. The first step is the calibration of the numerical model. The model shows better agreement with the measured post-storm profile with the following setup: non-hydrostatic assumption, wave breaking imposed by the sea surface instability, short-wave and long-wave interaction, avalanching, short wave stirring, no long wave stirring, long wave turbulence. The calibration factor for the avalanching module is 1.6 and the parameter related to the critical Shields number is 0.8. In what concerns the roughness coefficient, the Colebrook – White function has been used. The critical slopes for the wet and dry parts of the domain are 0.3 and 0.8. The maximum Courant number for the flow module is 0.4 for the Buival profile and 0.7 for the NR48 profile. Courant number has to be so restrictive because of the dense discretization of the beach profile. The morphological acceleration factor (Roelvink, 2006) is 5 for the Buival profile and 10 for the NR48 profile.

The XBeach model shows the least erosion along the NR48 profile, with these settings. The measurements show even light deposition, in the order of less than 20 cm, at 100 to 115 m along the post-storm profile, between elevations 1.2 and 0.9 m in the emerged zone, going towards the shoreline.

Along the Buival profile, the XBeach model shows deposition in the submerged part, at depths between -0.2 and -0.6 m. Differences in the elevations along the measured profile show deposition from few centimeters to 30 cm locally. The modeled post-storm Buival profile shows deposition going up to 20 cm.

Such differences are expected for a natural beach. Small deviations from the initial path of the profile might have occurred. We also must consider limitations of the XBeach model used in 1DH (profile mode). As stated by van Geer and Boers, 2012, when assessing dune erosion with a 1D model, sediment that erodes from the dune face is assumed to settle on the beach further offshore, without interacting with neighbouring transects. Eroded sediments from one transect may travel along the coastline and contribute to the amount of sediments in another transect.

Hence, there is no way to estimate the longshore contribution. In future submissions, we hope to use the same morphodynamic model, but in a 2DH approach. Estimations of the longshore contribution with mean wave climate can be found in Stănică et al, 2007.

The NR48 profile

The results of the XBeach simulations for the NR48 profile and all the storms considered are presented in Tables 2 to 4.

The sand volume changes are neglectible for the RP1_SE, regardless of the sea level, due to the lower wave heights.The sand volume changes are higher for the RP1_S and RP2_S storms than for the RP1_E and RP2_E storms, due to the higher wave heights from the Southern sector. For the RP5_S and RP5_E storms, the sand volume changes exceed 30% for MWL between 0.6 and 1 m.

Dune destruction occurs for the calculated sand volume changes over 30% (Figs. 4 and 5)

For the storms from the SE sector, the sand volume changes are significantly lower than for the storms from S and E.

Looking at the sand volume ratios with respect to the Return Periods, an assymptotic behaviour is noticed for all the storms considered, for MWL between 0 and 0.6 m (Fig. 6). For the SE storms, an increasing trend is noticed for MWL 0.8 m and 1 m. For the storms from the S sector, the assymptotic behaviour occurs also for MWL 0.8 m and the increasing trend can be observed only for MWL 1 m. For the storms from E, the assymptotic behaviour occurs for MWL 1 m, while the increasing trend can be noticed for MWL 0.8 m. The maximum sand volume erosion, exceeding 70%, occurs for MWL 0.8 m (Table 4 and Fig. 7 – storms E).

After reaching a maximum eroded sand volume, a decreasing trend with respect to MWL can be noticed, for the storms with lower Return Periods (Fig. 7), due to the diminished water velocity, for increased water level, and, thus, to less erosion. This happens for storms from SE and from S.

In the case of the RP10 storms from SE and S, the eroded sand volume keeps increasing with the water level (Fig. 7). This is due to the combined action of waves and SLR. For MWL 1 m, the eroded sand volume gets double for the RP10_S storm (63%) compared to the RP5_S storm (30.46%) (Table 3). For the RP10_SE storm the eroded sand volume reaches the highest value, over 7% (Table 2), but it is almost 9 times lower than in the case of the RP10_S storm, for which it reaches 63% (Table 3). The destruction of the dune is due to the increase of the significant wave heights for the storm from S, comparing to the one from SE (Table 1).

The RP10_E storm leads to a maximum eroded sand volume over 70% for the MWL of 0.8 m and a slight decrease to 66.7% for MWL 1 m (Table 4), due to more deposition occurring at increased MWL. This suggests an assymptotic behaviour with respect to the water level, that can also be noticed in Figure 7, for storms from E.

On the contrary, for the RP5_E storm, a general increase trend with respect to the MWL can be noticed (Fig. 7 - storms E). This is associated to the destruction of the inshore dune in the case of MWL 1 (Fig. 5).

For all the considered wave directions, the NR48 profile shows a change of the sand volume ratio slope at RP5 for a certain MWL value (Fig. 6) and at MWL 0.6 m for a certain RP value (Fig. 7). This change corresponds to a sand volume ra-

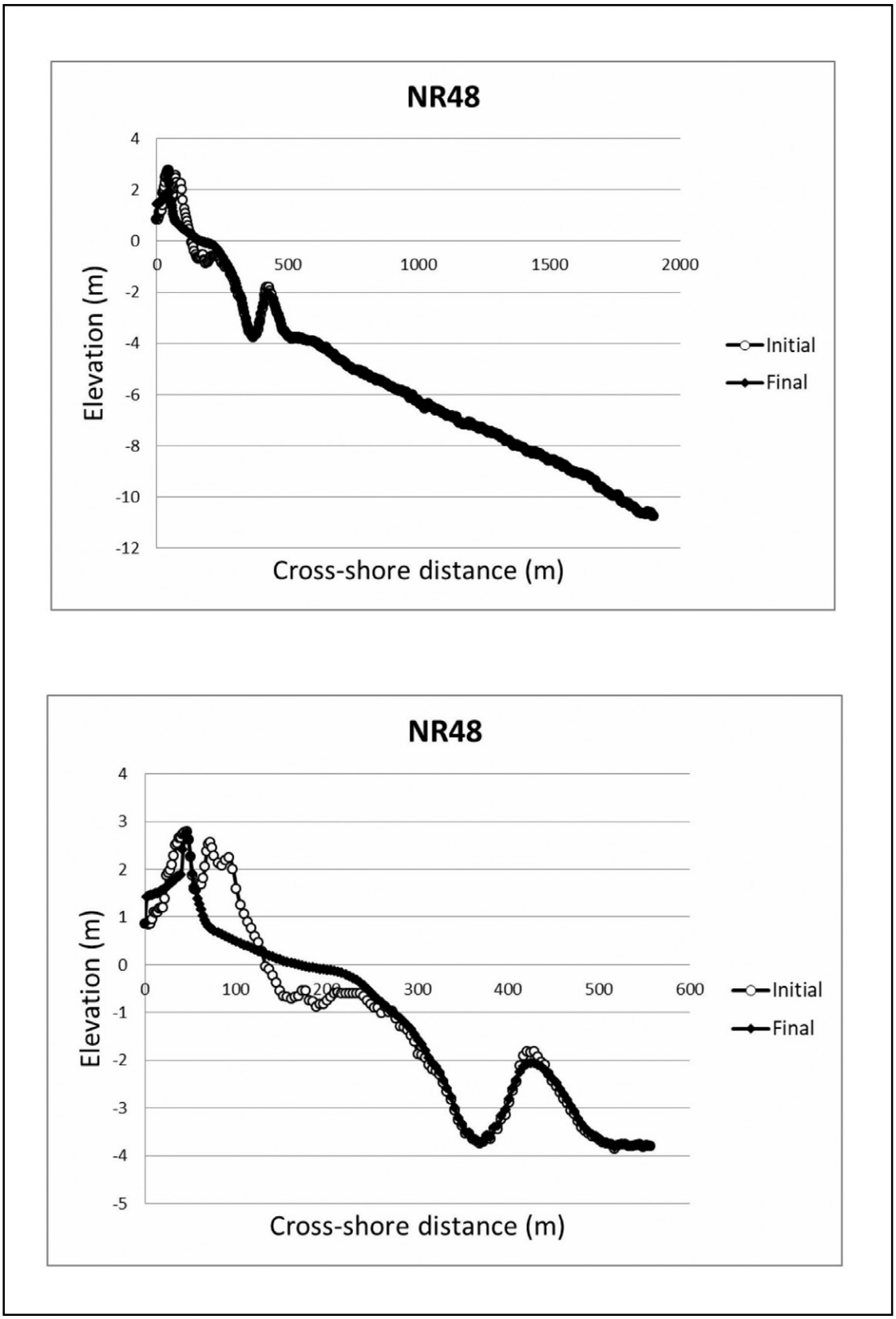

Fig. 4. NR48 profile – storm RP5 from South and MWL 0.8 m – full profile (up) and detail (down)

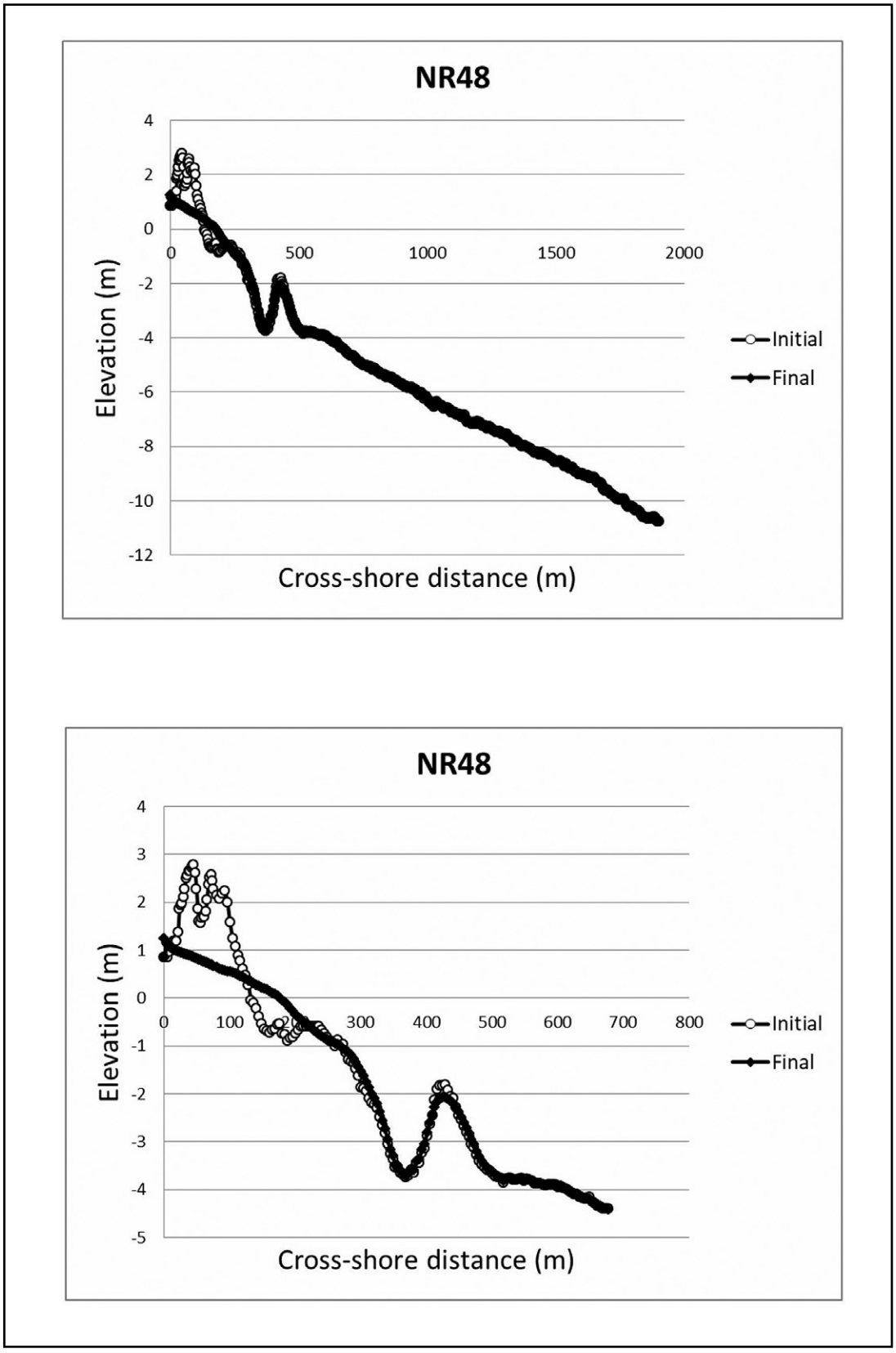

Fig. 5. NR48 profile – storm RP5 from East and MWL 1 m – full profile (up) and detail (down)

Table 2. Sand volume changes on the NR48 profile - storms from SE

RP_SE	Sand volume changes (%) MWL 0	Sand volume changes (%) MWL 0.2	Sand volume changes (%) MWL 0.4	Sand volume changes (%) MWL 0.6	Sand volume changes (%) MWL 0.8	Sand volume changes (%) MWL 1
RP1_SE	-0.0059	0.0034	0.0282	0.012	0.0005	0
RP2_SE	0.2073	0.8312	1.2351	1.0976	0.7461	0.4234
RP5_SE	2.1854	2.9503	2.8467	2.7528	2.2068	1.5793
RP10_SE	2.682	3.9791	3.2499	3.124	6.1252	7.3282

Table 3. Sand volume changes on the NR48 profile - storms from S

RP_S	Sand volume changes (%) MWL 0	Sand volume changes (%) MWL 0.2	Sand volume changes (%) MWL 0.4	Sand volume changes (%) MWL 0.6	Sand volume changes (%) MWL 0.8	Sand volume changes (%) MWL 1
RP1_S	0.2215	1.0139	1.1451	1.2732	0.6405	0.4029
RP2_S	4.3321	13.995	5.2716	15.1721	14.6544	13.9776
RP5_S	14.7086	19.3459	16.8653	32.0253	33.1704	30.4636
RP10_S	20.4635	19.8958	35.0956	36.2601	45.1826	63.0796

Table 4. Sand volume changes on the NR48 profile - storms from E

RP_E	Sand volume changes (%) MWL 0	Sand volume changes (%) MWL 0.2	Sand volume changes (%) MWL 0.4	Sand volume changes (%) MWL 0.6	Sand volume changes (%) MWL 0.8	Sand volume changes (%) MWL 1
RP1_E	0.0113	0.2876	0.5317	0.6266	0.234	0.1109
RP2_E	3.1892	4.5363	4.1541	4.1044	9.702	6.8422
RP5_E	18.3844	22.6018	17.3491	34.3076	33.39	55.6313
RP10_E	41.7054	38.3456	37.6684	38.0185	71.4399	60.6698

tio between 30% and 40%, for the storms from the Southern sector (Fig. 6)

Tables 5 to 7 show the resilience values for the NR48 profile for all the considered storms.

The mean slope ranges from: 0.0061 (RP10_S and MWL 1 m) and 0.0765 (RP2_S and MWL 0).

The mean runup ranges from: 0.18 m (RP10_S and MWL 1 m; RP5_E and MWL 1 m; RP10_E and MWL 0.8 m; RP10_E and MWL 1 m) and 0.37 m (RP2_S and MWL 0).

The mean elevation of the post-storm NR48 profile ranges from 0.3817m (RP2_S and MWL 0.6 m) and 0.8017 m (RP2_S and MWL 0).

The calculated resilience values for the NR48 profile are between 0.32 (RP10_E and MWL 0) and 2.55 (RP2_S and MWL 0.8).

For almost all the considered storms with MWL 0 and 0.2 m the RR values are less than 1. For MWL from 0.4 to 1 m, the RR values are higher than 1. There are few exceptions: RR less than 1 for RP1_SE and MWL 0.4 m and RR higher than 1 for RP2_S and MWL 0.2 m, and for RP10_S and MWL 0.2 m. In the RP1_SE case, this is due to the relatively low value of the highest significant wave height of 1.4 m (Table 1). In the RP2_S and RP10_S cases, this is due to the high values of the significant wave height from the S sector, of 3.4 m and 4.3 m, respectively (Table 1).

There are also RR values around or over 2, for higher RPs, of 5 and 10 year, and MWL 1 m. Usually, they are associated with storms with high maximum significant wave height, around 4 m. There are some exceptions: the RP2_S storm, with the maximum significant wave height of 3.4 m and MWL from 0.6 to 1 m, and the RP5_SE storm, with the maximum significant wave height of 2.6 m and MWL 1 m (Table 1), but leading to erosion of the profile and, therefore, to lower post-storm elevations (Table 5).

Simulations results for the NR48 profile

Table 5. Resilience values for the NR48 profile - storms from SE

RP_SE	MWL (m)	Mean elevation post-storm (m)	Mean slope	Runup (m)	Resilience Ratio
RP1_SE	0	0.7636	0.0506	0.29	0.38
	0.2	0.7627	0.0508	0.29	0.64
	0.4	0.7627	0.05	0.29	0.9
	0.6	0.7627	0.0505	0.29	1.17
	0.8	0.7629	0.0508	0.29	1.43
	1	0.7629	0.0508	0.29	1.69
RP2_SE	0	0.7499	0.051	0.29	0.39
	0.2	0.7147	0.0496	0.29	0.69
	0.4	0.5693	0.0428	0.27	1.18
	0.6	0.5867	0.0409	0.26	1.47
	0.8	0.6676	0.0421	0.27	1.6
	1	0.6725	0.0446	0.28	1.9
RP5_SE	0	0.7197	0.0589	0.32	0.44
	0.2	0.6617	0.0558	0.31	0.77
	0.4	0.5396	0.0431	0.27	1.24
	0.6	0.5118	0.0383	0.26	1.68
	0.8	0.5489	0.0379	0.26	1.93
	1	0.5732	0.0399	0.26	2.2
RP10_SE	0	0.7945	0.063	0.33	0.42
	0.2	0.5899	0.0555	0.31	0.86
	0.4	0.5173	0.0433	0.27	1.3
	0.6	0.4919	0.0383	0.26	1.75
	0.8	0.6522	0.0211	0.21	1.55
	1	0.6435	0.0232	0.22	1.9

Table 6. Resilience values for the NR48 profile - storms from S

RP_S	MWL (m)	Mean elevation post-storm (m)	Mean slope	Runup (m)	Resilience Ratio
RP1_S	0	0.7483	0.0515	0.29	0.39
	0.2	0.7036	0.0495	0.29	0.7
	0.4	0.5729	0.0429	0.27	1.17
	0.6	0.5828	0.0398	0.26	1.48
	0.8	0.6698	0.0429	0.27	1.6
	1	0.6728	0.0447	0.28	1.9
RP2_S	0	0.8017	0.0765	0.37	0.46
	0.2	0.4001	0.0444	0.27	1.17
	0.4	0.4451	0.049	0.29	1.55
	0.6	0.3817	0.0208	0.21	2.12
	0.8	0.3919	0.0158	0.2	2.55
	1	0.4815	0.0156	0.2	2.49

Table 6 (continued)

RP_S	MWL (m)	Mean elevation post-storm (m)	Mean slope	Runup (m)	Resilience Ratio
RP5_S	0	0.4883	0.0555	0.31	0.63
	0.2	0.5011	0.0453	0.28	0.96
	0.4	0.4453	0.0321	0.24	1.44
	0.6	0.5631	0.013	0.2	1.42
	0.8	0.5647	0.0144	0.2	1.77
	1	0.6029	0.0136	0.2	1.99
RP10_S	0	0.5191	0.0622	0.33	0.64
	0.2	0.4746	0.0446	0.28	1.01
	0.4	0.55	0.0144	0.2	1.09
	0.6	0.555	0.0162	0.2	1.44
	0.8	0.7108	0.0098	0.19	1.39
	1	0.5547	0.0061	0.18	2.13

Table 7. Resilience values for the NR48 profile - storms from E

RP_E	MWL (m)	Mean elevation post-storm (m)	Mean slope	Runup (m)	Resilience Ratio
RP1_E	0	0.7622	0.0508	0.29	0.38
	0.2	0.7465	0.0502	0.29	0.66
	0.4	0.6647	0.0438	0.27	1.01
	0.6	0.6702	0.0427	0.27	1.3
	0.8	0.6752	0.0458	0.28	1.6
	1	0.7603	0.0485	0.29	1.7
RP2_E	0	0.7568	0.0649	0.34	0.45
	0.2	0.6381	0.0644	0.33	0.83
	0.4	0.5146	0.0485	0.29	1.34
	0.6	0.4718	0.0428	0.27	1.84
	0.8	0.55	0.0201	0.21	1.84
	1	0.6929	0.0256	0.22	1.76
RP5_E	0	0.5591	0.0532	0.3	0.54
	0.2	0.4567	0.0358	0.25	0.99
	0.4	0.4013	0.0276	0.23	1.57
	0.6	0.604	0.0165	0.2	1.32
	0.8	0.554	0.0126	0.19	1.79
	1	0.5521	0.0064	0.18	2.14
RP10_E	0	0.7602	0.0299	0.24	0.32
	0.2	0.6546	0.0214	0.21	0.63
	0.4	0.555	0.0172	0.2	1.08
	0.6	0.5897	0.0188	0.21	1.37
	0.8	0.4769	0.0065	0.18	2.05
	1	0.6151	0.0066	0.18	1.92

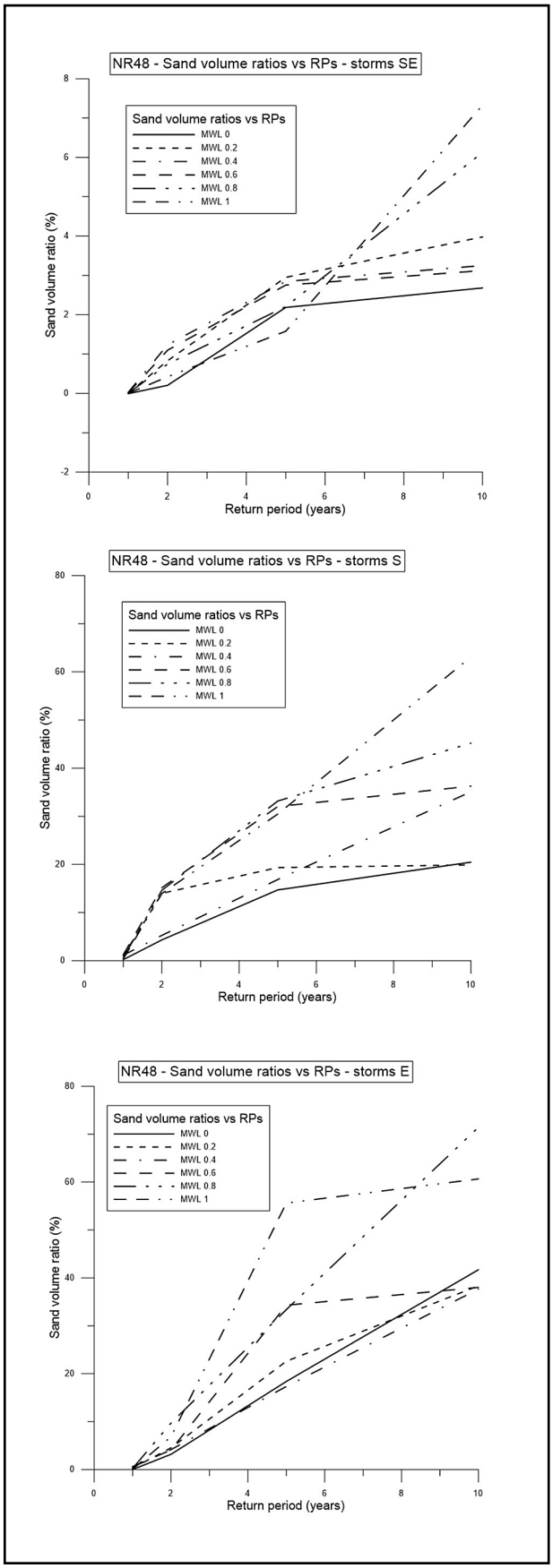

Fig. 6. NR48 profile – Sand volume ratios *vs* Return Periods for all the considered storms

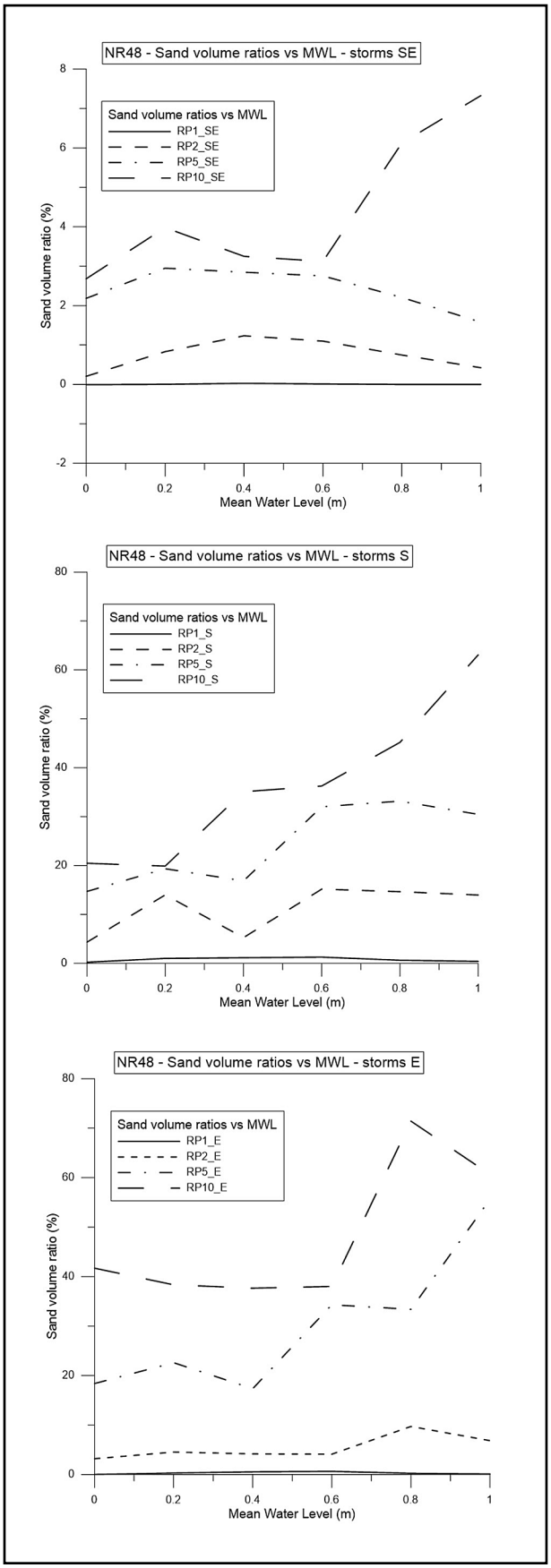

Fig. 7. NR48 profile – Sand volume ratios *vs* Mean Water Level for all the considered storms

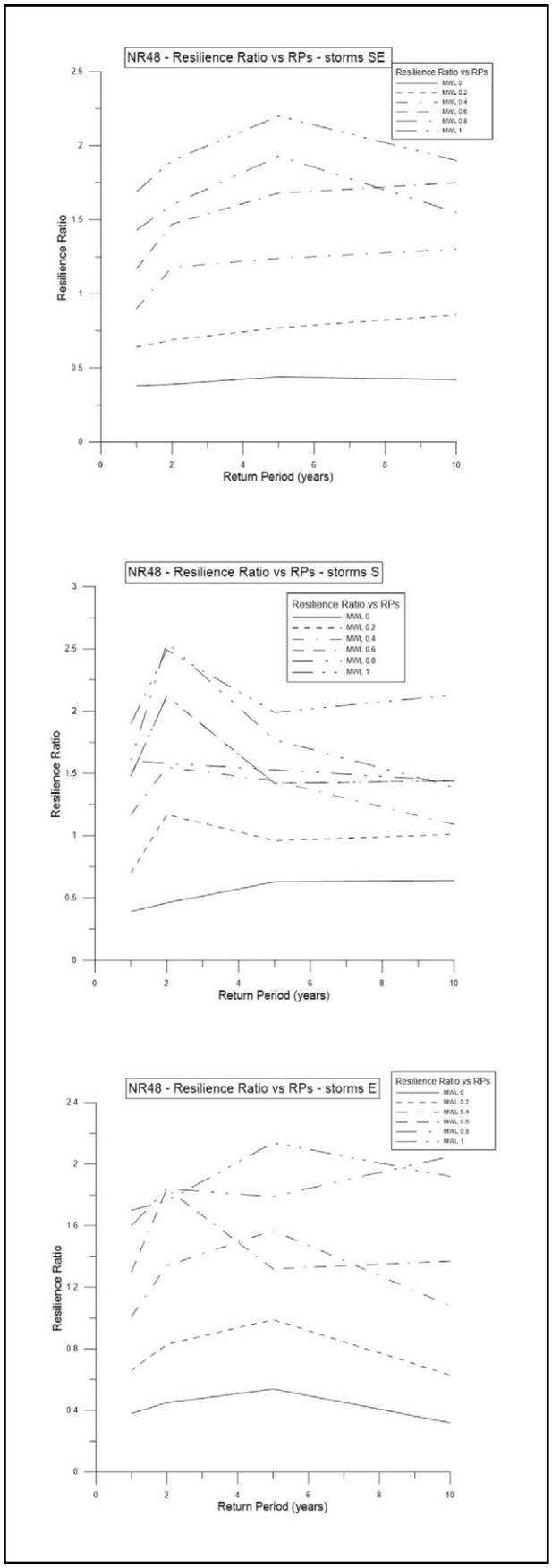

Fig. 8. NR48 profile – Resilience Ratio *vs* Return Periods for all the considered storms

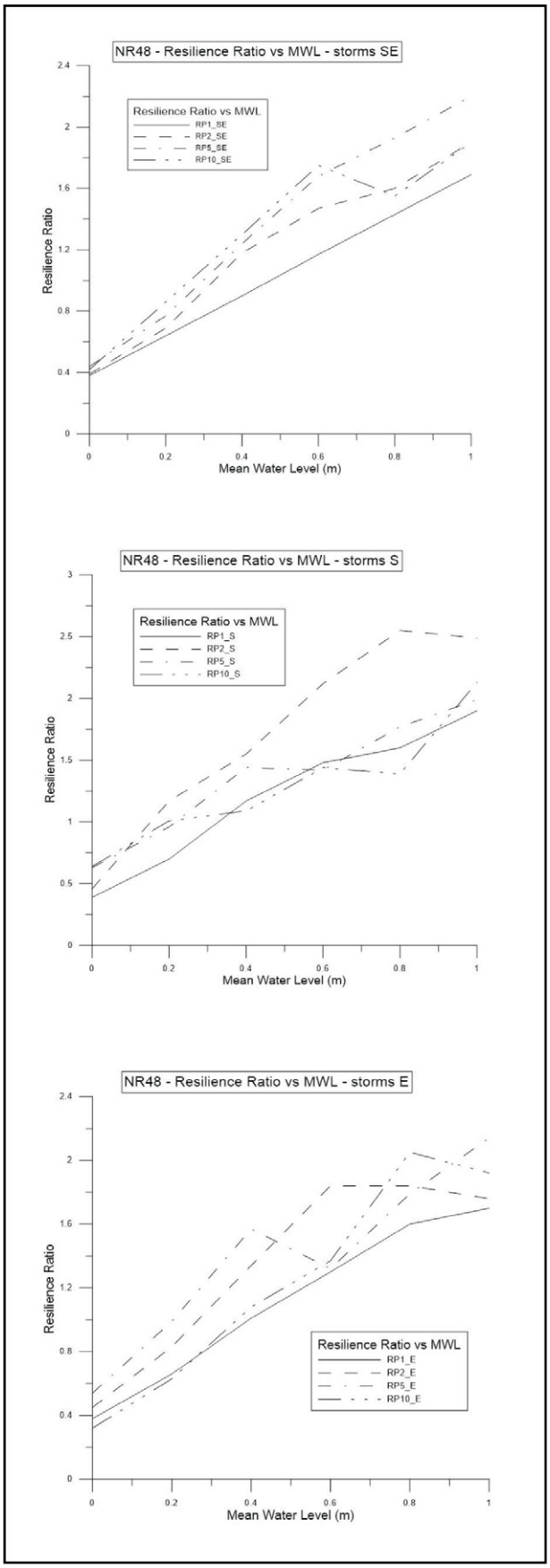

Fig. 9. NR48 profile – Resilience Ratio *vs* Mean Water Level for all the considered storms

The Buival profile

The results of the XBeach simulations for the Buival profile and all the storms considered are presented in the Tables 8 to 10.

Same as for the NR48 profile, the sand volume changes are neglectible for the RP1_SE, regardless of the sea level. This is due to the fact that waves from the SE have the lowest maximum wave heights. For RP1_S and RP2_S, the sand volume changes are higher than for RP1_E and RP2_E, respectively, as the maximum wave heights are higher for the storms from the Southern sector. For RP2_S, we notice sand volume changes over 25% for MWL between 0.4 and 1 m (Table 9).

The Buival profile shows assymptotic behaviour for the storms from the South sector, with the highest maximum wave heights (Fig. 12; storms from the S sector). There is no assymptotic behaviour for RP2_S and MWL 0.2 m, as the post-storm profile is not yet destroyed. Destruction occurs starting with MWL 0.4 m, when the sand volume change shows a maximum of 31.49% (Fig. 10).

Similarly to the NR48 profile, after reaching a maximum eroded sand volume, a decreasing trend with respect to MWL can be noticed (Fig. 13), due to the fact that, as the sea level increases, the water velocity is lower, thus resulting in less erosion. Increased sea level but also higher waves lead to the collapse of the dunes in the emerged part (Figs. 10 and 11).

Assymptotic behaviour can also be noticed for RP5_S and RP5_E, for MWL starting with 0.2 m (Fig. 13).

The Buival profile shows more variability than the NR48 profile, due to the influence of the Sf. Gheorghe distributary.

Tables 11 to 13 show the resilience values for the Buival profile for all the considered storms.

The mean slope ranges from: 0.0046 (RP10_E and MWL 0) and 0.0416 (RP2_S and MWL 0).

The mean runup ranges from: 0.18 m (RP2_S and MWL 0.4 to 1 m; RP5_S and MWL 0.4 to 1 m; RP10_S and MWL 0.4 to 1 m; RP5_E and MWL 0.8 to 1 m; RP10_E and MWL 0; RP10_E and MWL 0.4 to 1 m) and 0.27 m (RP2_S and MWL 0).

The mean elevation of the post-storm Buival profile ranges from 0.3917 m (RP2_S and MWL 0.2 m) and 0.911 m (RP10_SE and MWL 1 m).

The calculated resilience values for the Buival profile are between 0.25 (RP10_E and MWL 0) and 2.43 (RP10_E and MWL 1 m). They are almost of the same order as the ones calculated for the NR48 profile.

Similarly to the NR48 profile, for almost all the considered storms with MWL 0 and 0.2 m, the RR values are less than 1. For MWL from 0.4 to 1 m, the RR values are higher than 1. Same as for NR48, and for the same reasons, there are two exceptions: RR less than 1 for RP1_SE and MWL 0.4 m, and RR higher than 1 for RP2_S and MWL 0.2 m.

RR values are over 2 only for the RP10_E storm with MWL 0.8 - 1 m, which has the highest significant wave height, of 4.45 m (Table 1).

Simulations results for the Buival profile

Table 8. Sand volume changes on the Buival profile - storms from SE

RP_SE	Sand volume changes (%) MWL 0	Sand volume changes (%) MWL 0.2	Sand volume changes (%) MWL 0.4	Sand volume changes (%) MWL 0.6	Sand volume changes (%) MWL 0.8	Sand volume changes (%) MWL 1
RP1_SE	0.0101	0.4743	0.0267	0.0045	0.0002	0.0001
RP2_SE	0.5506	1.5364	1.7193	1.6642	0.7517	0.2794
RP5_SE	3.815	5.2615	4.9273	4.4176	3.6835	2.7598
RP10_SE	4.8091	5.4403	5.5169	5.6034	10.1768	8.457

Table 9. Sand volume changes on the Buival profile - storms from S

RP_S	Sand volume changes (%) MWL 0	Sand volume changes (%) MWL 0.2	Sand volume changes (%) MWL 0.4	Sand volume changes (%) MWL 0.6	Sand volume changes (%) MWL 0.8	Sand volume changes (%) MWL 1
RP1_S	0.0101	1.5477	2.0696	1.5479	0.7738	0.2736
RP2_S	9.9128	10.3319	31.4909	29.9432	28.8982	25.7835
RP5_S	12.0596	35.9231	35.4118	35.6534	32.4456	36.5168
RP10_S	43.412	46.9417	47.8462	44.8234	46.8425	45.7485

Table 10. Sand volume changes on the Buival profile - storms from E

RP_E	Sand volume changes (%) MWL 0	Sand volume changes (%) MWL 0.2	Sand volume changes (%) MWL 0.4	Sand volume changes (%) MWL 0.6	Sand volume changes (%) MWL 0.8	Sand volume changes (%) MWL 1
RP1_E	0.2254	0.9551	0.8521	0.7379	0.1416	0.0521
RP2_E	5.832	6.468	7.0438	6.8015	6.2912	17.4529
RP5_E	23.4591	38.7373	38.7316	35.9973	37.0778	41.226
RP10_E	51.9695	52.5406	49.4187	56.2049	57.4968	55.5975

Table 11. Resilience values for the Buival profile - storms from SE

RP_SE	MWL (m)	Mean elevation post-storm (m)	Mean slope	Runup (m)	Resilience Ratio
RP1_SE	0	0.675	0.0308	0.24	0.36
	0.2	0.6756	0.0303	0.24	0.65
	0.4	0.6733	0.0299	0.24	0.95
	0.6	0.675	0.0304	0.24	1.24
	0.8	0.6757	0.0305	0.24	1.54
	1	0.6757	0.0304	0.24	1.84
RP2_SE	0	0.6845	0.0323	0.24	0.35
	0.2	0.5681	0.0269	0.23	0.76
	0.4	0.5184	0.0232	0.22	1.2
	0.6	0.5246	0.0247	0.22	1.56
	0.8	0.6424	0.0266	0.23	1.6
	1	0.7247	0.0262	0.23	1.7
RP5_SE	0	0.5736	0.0371	0.25	0.44
	0.2	0.4459	0.0296	0.23	0.96
	0.4	0.462	0.0243	0.22	1.34
	0.6	0.4653	0.02	0.21	1.74
	0.8	0.5658	0.0214	0.21	1.79
	1	0.6716	0.0199	0.21	1.8
RP10_SE	0	0.7179	0.0367	0.25	0.35
	0.2	0.4572	0.0271	0.23	0.94
	0.4	0.5711	0.0252	0.22	1.09
	0.6	0.5535	0.0235	0.22	1.48
	0.8	0.7749	0.0124	0.19	1.28
	1	0.911	0.0155	0.2	1.32

Table 12. Resilience values for the Buival profile - storms from S

RP_S	MWL (m)	Mean elevation post-storm (m)	Mean slope	Runup (m)	Resilience Ratio
RP1_S	0	0.675	0.0308	0.24	0.36
	0.2	0.5657	0.0278	0.23	0.76
	0.4	0.5037	0.0227	0.22	1.23
	0.6	0.5567	0.0227	0.22	1.47
	0.8	0.6405	0.0267	0.23	1.61
	1	0.7541	0.0276	0.23	1.63
RP2_S	0	0.5031	0.0416	0.27	0.54

Table 12 (continued)

RP_S	MWL (m)	Mean elevation post-storm (m)	Mean slope	Runup (m)	Resilience Ratio
	0.2	0.3917	0.0297	0.24	1.12
	0.4	0.5507	0.0074	0.18	1.05
	0.6	0.5915	0.0073	0.18	1.32
	0.8	0.6227	0.0075	0.18	1.57
	1	0.8301	0.0079	0.18	1.42
RP5_S	0	0.4789	0.0404	0.26	0.54
	0.2	0.5033	0.0083	0.19	0.77
	0.4	0.4714	0.0069	0.18	1.23
	0.6	0.4774	0.0069	0.18	1.63
	0.8	0.6863	0.0072	0.18	1.43
	1	0.679	0.0067	0.18	1.74
RP10_S	0	0.503	0.0131	0.2	0.4
	0.2	0.4365	0.0089	0.19	0.89
	0.4	0.4707	0.0074	0.18	1.23
	0.6	0.5283	0.0062	0.18	1.48
	0.8	0.5676	0.0054	0.18	1.73
	1	0.6226	0.0065	0.18	1.9

Table 13. Resilience values for the Buival profile - storms from E

RP_E	MWL (m)	Mean elevation post-storm (m)	Mean slope	Runup (m)	Resilience Ratio
RP1_E	0	0.7017	0.0313	0.24	0.34
	0.2	0.5706	0.0252	0.22	0.74
	0.4	0.5806	0.025	0.22	1.07
	0.6	0.5824	0.0263	0.23	1.43
	0.8	0.634	0.0277	0.23	1.62
	1	0.7052	0.0273	0.23	1.74
RP2_E	0	0.6139	0.0388	0.26	0.42
	0.2	0.4291	0.029	0.23	1
	0.4	0.4358	0.0249	0.22	1.42
	0.6	0.4763	0.0224	0.22	1.72
	0.8	0.5678	0.0173	0.21	1.78
	1	0.8667	0.009	0.19	1.37
RP5_E	0	0.5806	0.0185	0.21	0.36
	0.2	0.506	0.01	0.19	0.77
	0.4	0.4803	0.0089	0.19	1.23
	0.6	0.5145	0.0082	0.19	1.54
	0.8	0.6487	0.0065	0.18	1.51
	1	0.6552	0.0064	0.18	1.8
RP10_E	0	0.7148	0.0046	0.18	0.25
	0.2	0.4951	0.0111	0.19	0.79
	0.4	0.5483	0.0078	0.18	1.06
	0.6	0.4651	0.0059	0.18	1.68
	0.8	0.4217	0.0055	0.18	2.32
	1	0.4851	0.0059	0.18	2.43

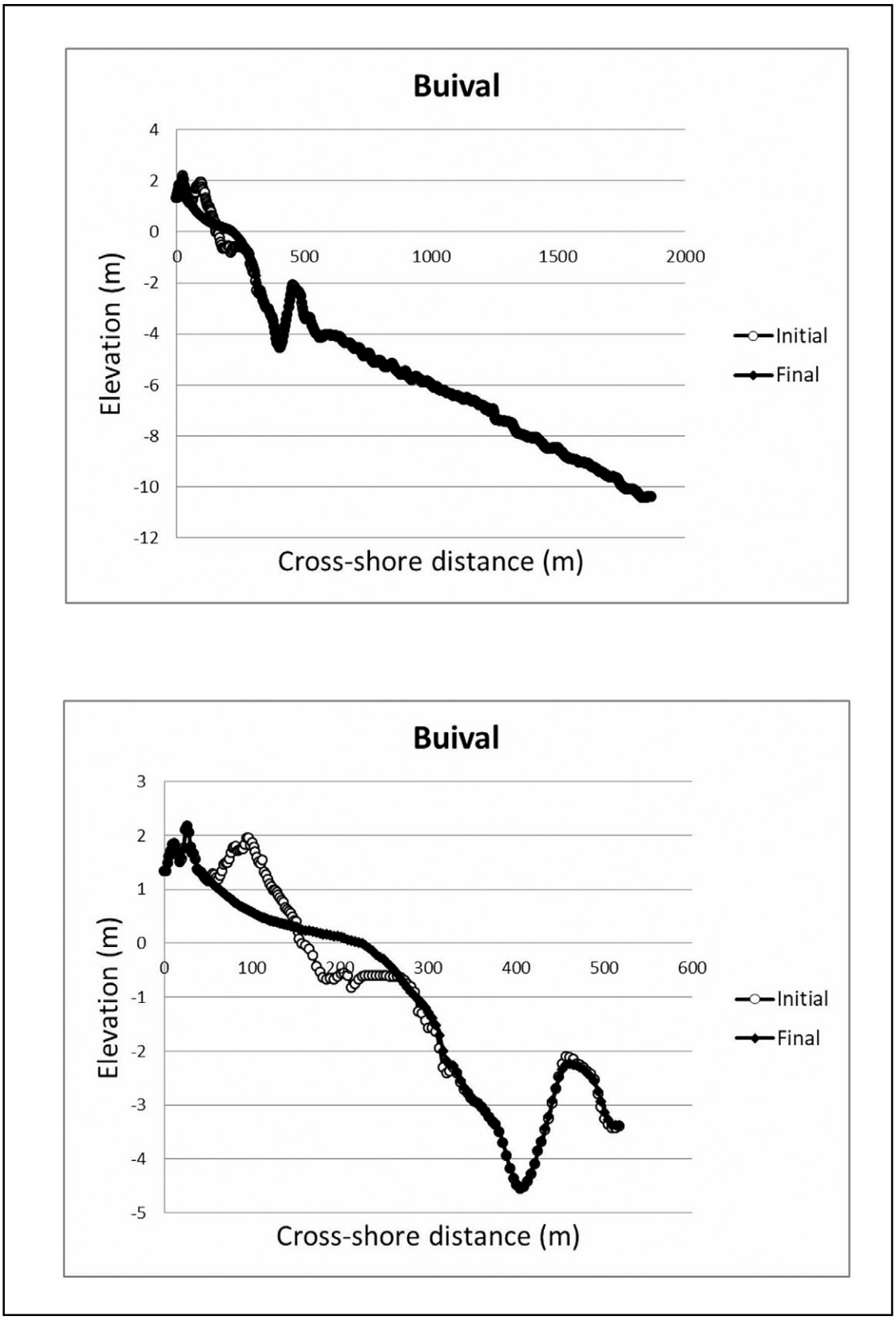

Fig. 10. Buival profile – storm RP2 from South and MWL 0.4 m – full profile (up) and detail (down)

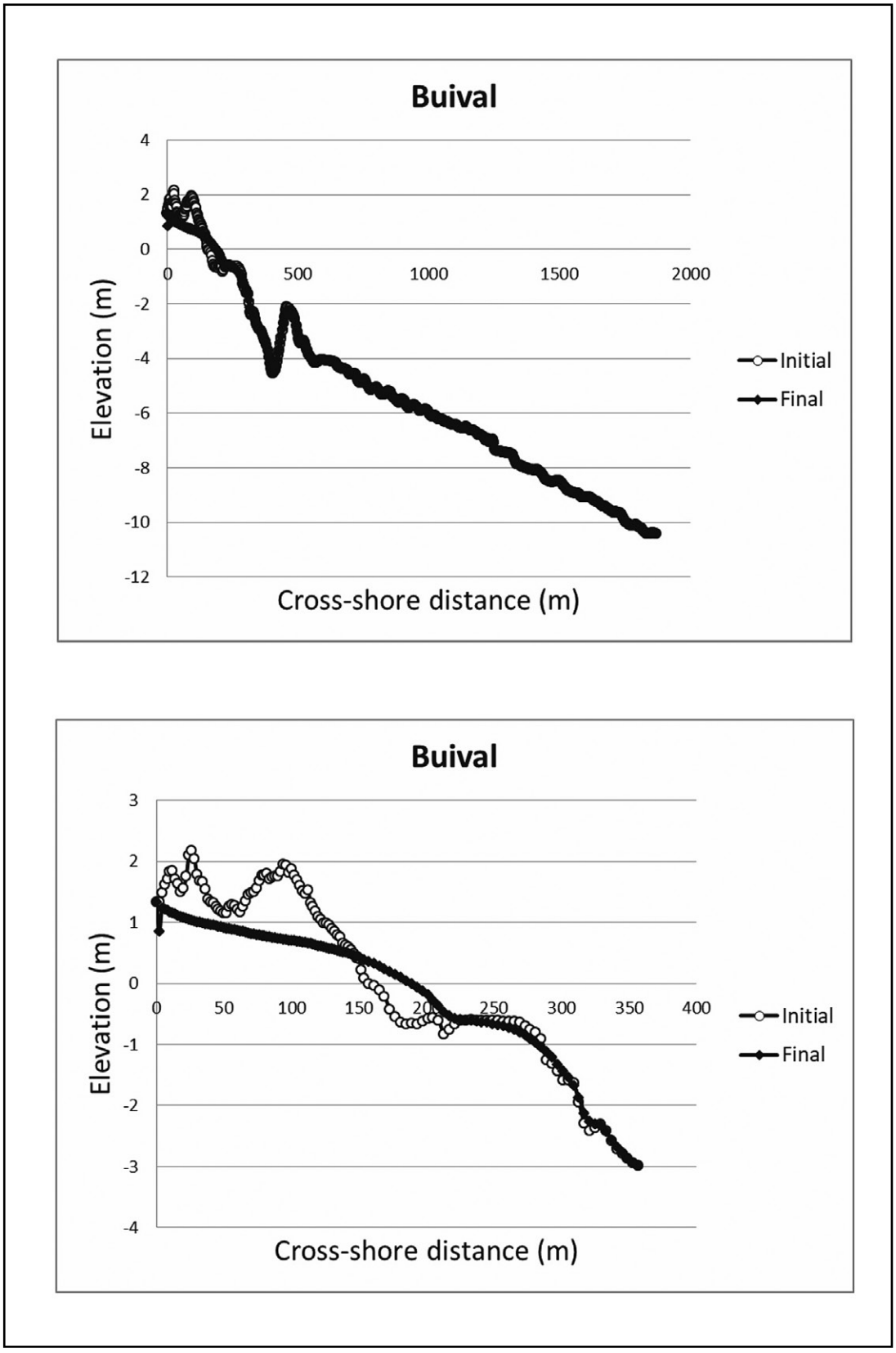

Fig. 11. Buival profile – storm RP5 from East and MWL 1 m – full profile (up) and detail (down)

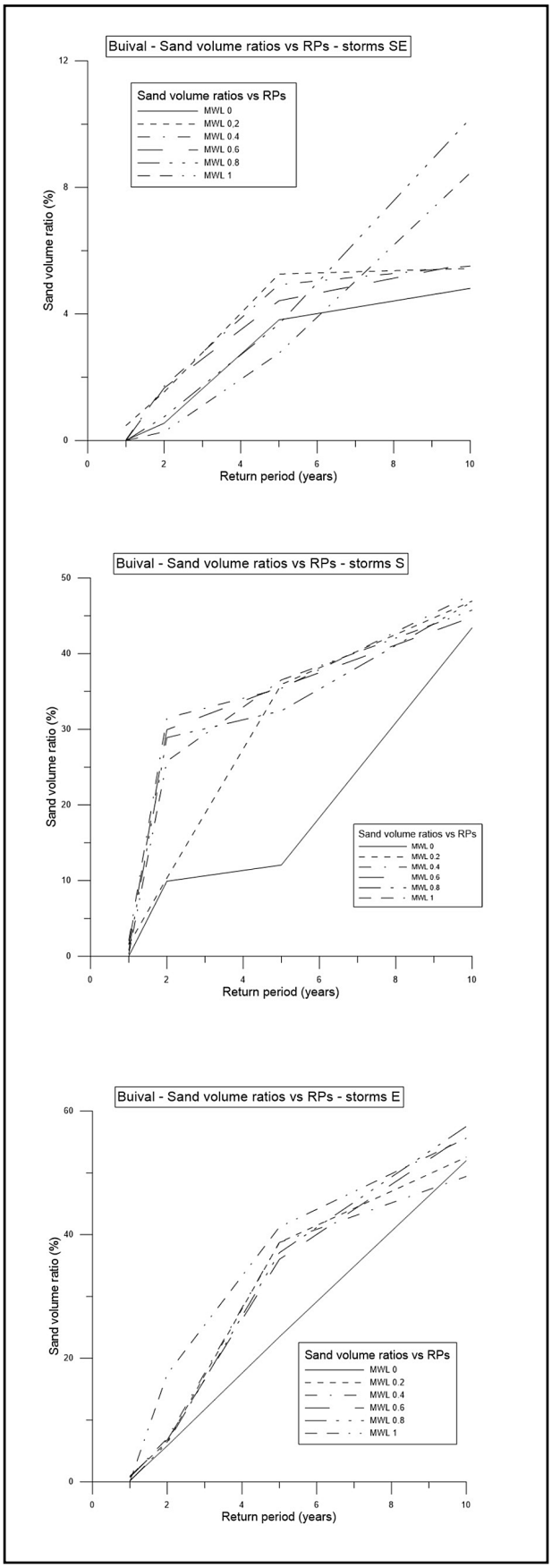

Fig. 12. Buival profile – Sand volume ratios *vs* Return Periods for all the considered storms

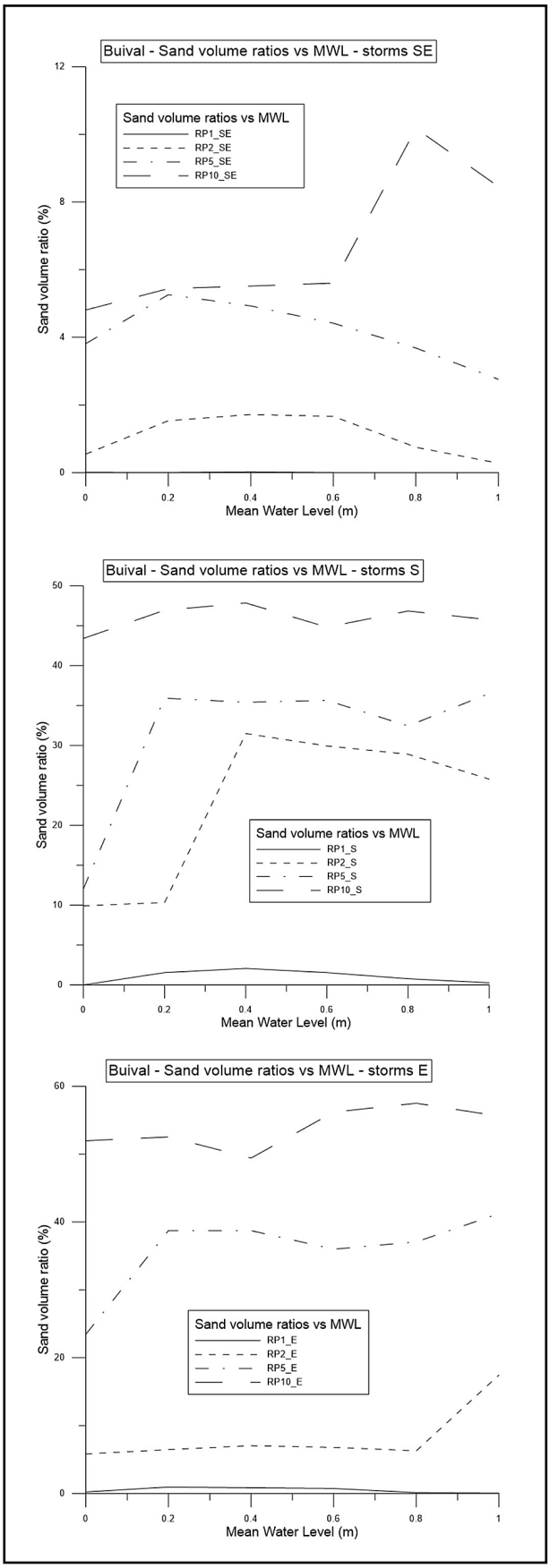

Fig. 13. Buival profile – Sand volume ratios *vs* Mean Water Level for all the considered storms

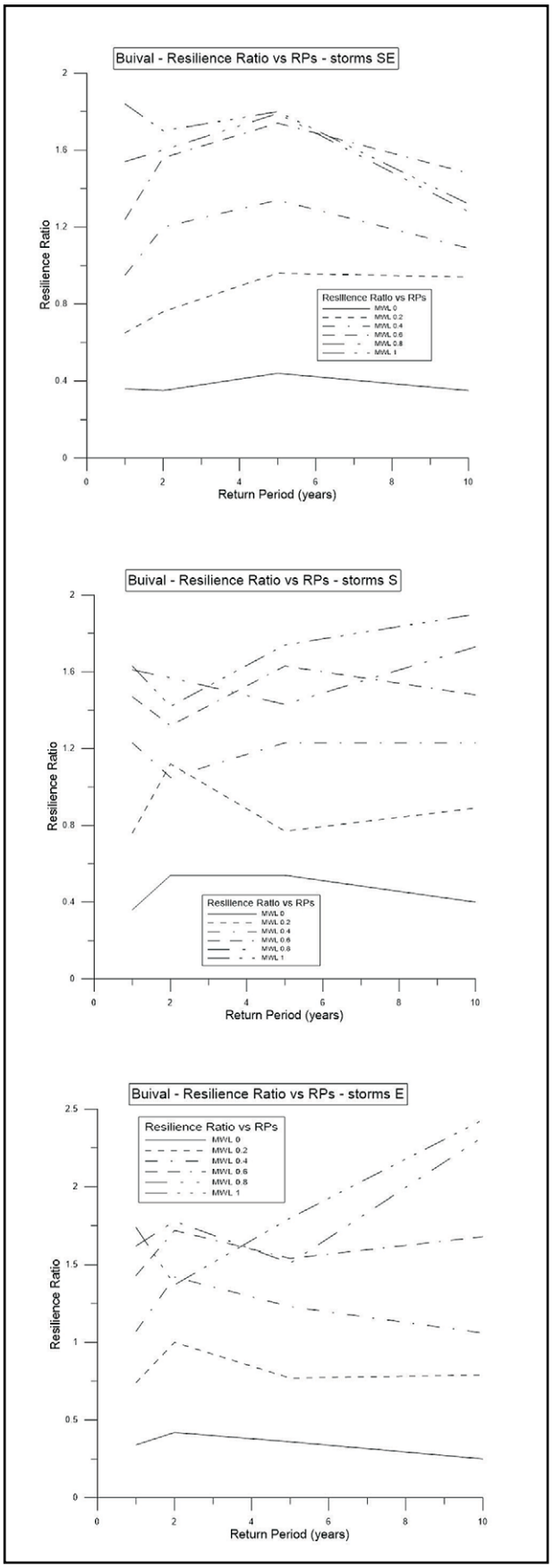

Fig. 14. Buival profile – Resilience Ratio *vs* Return Periods for all the considered storms

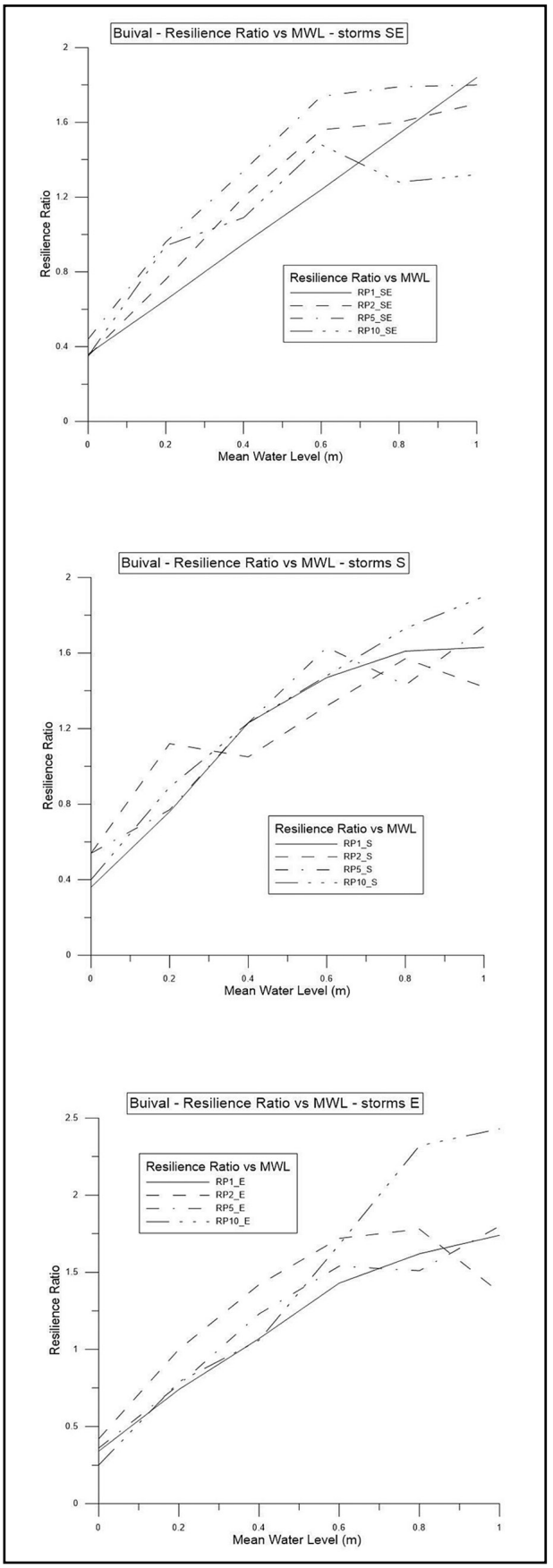

Fig. 15. Buival profile – Resilience Ratio *vs* Mean Water Level for all the considered storms

4. DISCUSSION

Low energetic waves (SE) and high sea levels lead to mass exchange from the inshoreward area to the present upper swash zone, that is permanently flooded by the SLR. For this reason, the erosion values are near zero. The post-storm beach profiles show essentially a predominant collision regime (Sallenger, 2000).

More energetic waves (E and S) and high sea levels lead to the collapse of the emerged dune, corresponding to the inundation regime on the Storm Impact Scale (Sallenger, 2000). In this case, the magnitude of the return flow induced by the waves is enough to mobilise the sediment offshorewards. The eroded volume tends to be accumulated at the lower swash zone (near 0 to -2 m water depth). The sediment is eroded and deposited at higher depth, thus leading to a re-shaping of the profile and to a deficit between the emerged and submerged parts.

It is concluded that the effect of SLR exacerbates erosion when combined with energetic waves. The beach system shows higher Resilience Ratios, as they increase both with SLR and, at the same time, as the post-storm elevation is lower, due to erosion. Moreover, at higher SLR, a more accelerated pace of land loss is expected. However, under low energetic conditions, the effect is not as dramatic.

In our analysis, we have been looking at the results of the simulations in order to find an „assymptotic behaviour" of the profile. This means that the eroded sand volume tends to reach a maximum value with respect to the SLR and to the intensity of the storm. Starting from a certain MWL or from a certain RP of the storm, the eroded sand volume is not expected to change significantly.

The RR indicator is used to analyze the effects of various storms. The analysis carried out herein shows that higher RR are related to higher RP and higher MWL. This was expected, as stronger storms may lead to more destruction. However, sometimes, a storm with lower RP may lead to high RR, depending on the wave height and direction. The morphological characteristics of the profiles also play an important role in the response to the forcings.

Even if it has not been performed on a wide area, this study shows that a coast does not respond in the same way, on its whole length, to the same type of forcing. Therefore, similar analyses, carried out on several profiles, may prove useful and provide more realistic results.

The analysis based on extreme storms may provide a certain trend for the metric that we use. The extreme storms are less likely to occur. But if a storm with lower wave heights occurs, a quick estimation of the sand volume change or of the RR value could be done by following the trend of the analyzed metric.

The sand volume change, as well as the Resilience Ratio can be used in setting up Tipping Points in our 1D analysis. It is a simplified approach, as it is based on 1D modelling, but it can provide a quick and easy way to estimate the state of the coast for extreme storms on individual beach profiles.

Setting up Tipping Points

Assessment of Tipping Points should be carried out on every individual profile, considering highly energetic conditions.

Every profile represents a specific case. Therefore, the analysis should consider both the pre-storm and post-storm profiles, as well as the specific eroded sand volumes.The profiles used in this analysis show specific behaviour, even if they are rather close and exposed to the same storms.

The sand volume change following an extreme storm could be used as a Tipping Point for the beach profile behaviour, as it expresses the maximum damage to be expected as effect of the action of drivers.

The NR48 profile

Following an extreme storm, the profiles may be reshaped, as it is the case for the NR48 profile and the storms with 5 years RP, from East and South and MWL starting with 0.6 m. Destruction of the seaward dune of the NR48 profile occurs for the storm with 5 years RP from East and South and MWL 0.6 m. Both dunes along the NR48 profile may be destroyed by the storm with 5 years RP from East and MWL 1 m (Fig. 5). The landward dune is not destroyed with the storm with 5 years RP from South and MWL 1 m.

Summarizing the results for NR48 profile, we notice that, for the RP5_S storm with MWL 0.8, the first dune has already been destroyed (Fig. 4). Table 1 shows that, for RP5, the storm from the Southern sector has the highest significant wave height. Destruction of the first dune is associated to a sand volume change of 33.17% (Table 3). Figure 7 shows an assymptotic behaviour of the sand volume change for the RP5 storms from the Southern sector, starting with MWL 0.6 m. Table 3 shows values around 30% even at higher MWL. In this way, the sand volume change of 30% could be a Tipping Point for the NR48 profile.

For the RP5 storms from the Eastern sector, the sand volume change increases as MWL gets higher than 0.6 m. Thus, we can infer that MWL of 0.6 m could also be a Tipping Point for the NR48 profile.

The calculated RR values for the RP5 storms with MWL 0.6 m are between 1.32 for the Eastern sector (Table 7) and 1.68 for the Southeastern sector (Table 5). Figure 8 shows that the calculated values RR have an assymptotic behaviour for MWL 0.6 m, for the storms with higher RP. Therefore, we can infer that the RR value of 1.5 could also be a Tipping Point for the NR48 profile.

The Buival profile

The Buival profile is re-shaped by the storms with 2 years RP from East, but the seaward dune is destroyed for MWL 1 m.

In the case of the storm with 2 years RP from South, the seaward dune along the Buival profile is destroyed at MWL 0.4 m (Fig. 10). In the case of an extreme storm with 5 years RP from East coupled with MWL 0 and one with 5 years RP from S with MWL 0.2 m, the seaward dune is destroyed. Both dunes along the Buival profile may be destroyed by the storm with 2 years RP from South and MWL 1 m and by the storms with 5 years RP from East and South and MWL 0.8 m.

Summarizing the results for the Buival profile, we notice that, for the RP2_S storm with MWL 0.4, the first dune has already been destroyed (Fig. 10). Table 1 shows that, for RP2, the storms from the Southern sector have the highest significant wave height. Destruction of the first dune along the Buival profile is associated to a sand volume change of 31.49% (Table 9). The highest values for the sand volume ratio, for the RP2 storms, are the ones from the Southern sector around 30%, with assymptotic behaviour at higher MWL (Table 9 and Fig. 13). The sand volume change of 30% could be a Tipping Point also for the Buival profile, as well as the MWL of 0.4 m.

The calculated RR values for the RP2 storms with MWL 0.4 m are between 1.05 for the Southern sector (Table 12) and 1.42 for the Eastern sector (Table 13). Thus, we can consider that the RR value of 1 could also be a Tipping Point for the Buival profile.

Following this analysis, one can conclude that every beach profile should be specifically treated. Drivers such as waves and SLR have to be incorporated in the analysis, together with the morphology and the grain size, as they have a direct impact on the erosion and deposition along the beach profile. Moreover, two profiles located rather close to each other may behave differently at the same storm, due to the local morphology and the grain size. For this reason, specific analysis should be performed on every beach profile.

The analysis we propose can be applied on natural sandy beaches, where sediment dynamics is driven by the direct action of waves. The profiles used for this analysis are located on a pristine coast, where no buildings or touristic development are foreseen.

Moreover, if nature-based solutions are foreseen for coastal protection, this kind of analysis should be repeated and the metrics used, such as the sand volume ratio and the Resilience Ratio should be calculated for the new hydrodynamic conditions.

In order to perform a better morphology survey, remote sensing and video image (Valentini *et al.*, 2017) are promising techniques to measure run-up and the emerged beach. That would pave the way for long-term monitoring which is precisely one of the most pressing urges in marine geomorphology research.

CONCLUSIONS

A morphodynamic model at the Danube Delta coast has been set-up and calibrated with real data and a recent storm.

The impact under different extreme storms conditions, assessed for wave return periods ranging from 1 to 10 years, and Sea Level Rise ranging from 0 to 1 m has been conducted. This analysis provided the sand volume changes for every extreme storm represented herein, as well as the conditions for which the profiles could be destroyed.

In our analysis we have attempted to detect assymptotic behaviour of the analyzed profiles with respect to drivers. Thus, we could estimate the most important part of the damage occurring to the analyzed profiles, under severe conditions. The response is interesting for the management of the Danube Delta Biosphere Reserve, taking into account the present-day challenges represented by the climate change.

At the same time, this study can provide answers to what happens in the case of moderate storms, that are most likely to occur. The response of a moderate storm could be implicitely included in this type of analysis, knowing that the drivers would, most probably, be lower than the ones considered herein.

The proposed methodology can be useful for detecting Tipping Points. As inferred from this study, these are depending on the local scale conditions. Assessing the effect of a storm should be carried out on individual beach profiles, in order to have a realistic response, involving the local-scale particularities.

The methodology proposed in this paper can be applied both in natural environments and on more urbanized coasts, as well as for analyzing measures for coastal protection.

ACKNOWLEDGEMENTS

This work has been started within the FP7 RISES-AM project (GA 603396), funded by the European Union, and completed within the PN 16450202, as part of the DELMAR project, Contract no. 45N/2016, funded by the Romanian Authority for Scientific Research. We are grateful to Dr. Florin Tătui from University of Bucharest, Faculty of Geography, for providing the beach profile data, which allowed us to carry out this study.

REFERENCES

Arkhipkin V.S., Gippius F. N. , Koltermann K. P., Surkova G. V., 2014 - Wind waves in the Black Sea: results of a hindcast study. *Nat. Hazards Earth Syst. Sci.*, 14, 2883–2897, 2014. www.nat-hazards-earth-syst-sci.net/14/2883/2014/ doi:10.5194/nhess-14-2883-2014

Bajo M., Ferrarin C., Dinu I., Umgiesser G., Stănică A. 2014 - The water circulation near the Danube Delta and the Romanian coast modelled with finite elements. *Continental Shelf Research*, 78(2014), p. 62 – 74.

Bhattacharya J.P., Giosan L., 2003 - Wave-influenced deltas: geomorphologic implications for facies reconstruction, *Sedimentology*, 50, 187-210.

Bondar C., Panin N., 2001 – The Danube Delta hydrologic data base and modelling. *Geo-Eco-Marina*, 5-6, Bucharest - Constanta, Romania, p. 5 – 52.

Booij N., Ris R.C., Holthuijsen L.H., 1999. A third-generation wave model for coastal regions, Part I, Model description and validation. *Journal of Geophysical Research*, 104 (C4): 7649-7666.

Chiaia G., Damiani L., Petrillo A., 1992 - Evolution of a beach with and without a submerged breakwater: Experimental investigation - 23nd ICCE., Venice, October 1992

Dan S., Stive M.J.F., Walstra D.J., Panin N., 2009 – Wave climate, coastal sediment budget and shoreline changes for the Danube Delta. *Marine Geology*, 262, issues 1-4, p. 39 – 49.

Dan S., 2013 – Coastal Dynamics of the Danube Delta. Ph.D. thesis, Delft University of Technology

Giosan L., Bokuniewicz H., Panin N., Postolache I., 1999 – Longshore Sediment Transport Pattern along the Romanian Danube Delta Coast. *Journal of Coastal Research*, 15 (4), p. 859 – 871.

Gràcia V., García-Leon M., Grifoll M., Sánchez-Arcilla A., 2013. Breaching of a barrier under extreme events: the role of morphodynamic simulations. *Journal of Coastal Research* (Special Issue 65): 951-956.

HALCROW UK *et al*. (2011-2012) – Master Plan "Protection and rehabilitation of the coastal zone".

Hinkel J, Jaeger C., Nicholls R.J., Lowe J., Renn O., Peijun P., 2015 - Sea-level rise scenarios and coastal risk management, *Nature Climate Change*, 5, 188-190

IPCC WG1, 2013 - *Climate Change 2013: The Physical Science Basis*. IPCC Working Group I Contribution to AR5; Cambridge University Press, Cambridge, UK and New York, USA, pp. 1029:1136.

Jevrejeva S., Grinsted A., Moore J.C., 2014 - Upper limit for sea level projections by 2100. *Environmental Research Letters*, 9(10): 104008.

Johnson H., 2011 - Wave Modelling Report. Reduction of Coastal Erosion on the Black Sea Coast. Master Plan "Protection and rehabilitation of the coastal zone".

Kovats, R.S., R. Valentini, L.M. Bouwer, E. Georgopoulou, D. Jacob, E. Martin, M. Rounsevell, and J.-F. Soussana, 2014: Europe. In: *Climate Change 2014: Impacts, Adaptation, and Vulnerability. Part B: Regional Aspects. Contribution of Working Group II to the Fifth Assessment Report of the Intergovernmental Panel on Climate Change* [Barros, V.R., C.B. Field, D.J. Dokken, M.D. Mastrandrea, K.J. Mach, T.E. Bilir, M. Chatterjee, K.L. Ebi, Y .O. Estrada, R.C. Genova, B. Girma, E.S. Kissel, A.N. Levy, S. MacCracken, P .R. Mastrandrea, and L.L. White (eds.)]. Cambridge University Press, Cambridge, United Kingdom and New York, NY , USA, pp. 1267-1326.

Lesser G.R., Roelvink J.A., van Kester J.A.T.M., Stelling G.S., 2004. Development and validation of a three-dimensional morphological model. *Coastal Engineering*, 51(8-9): 883 - 915.

Lisi, I., Molfetta, M.G., Bruno, M.F., Di Risio, M., Damiani, L., 2013. Morphodynamic classification of sandy beaches in enclosed basins: The case study of Alimini (Italy) - *Journal of Coastal Research*, SPEC. ISSUE 64, 2011, Pages 180-184 ISSN: 07490208

Panin N., 1996 – Impact of global changes on geo-environmental and coastal zone state of the Black Sea. *Geo-eco-marina*, 1, p. 7 – 23,

Panin N., 1998 – *Danube Delta: Geology, Sedimentology, Evolution.* Association des Sédimentologistes Français, Paris, 65 p.

Panin N., 1999 – Global changes, sea level rise and the Danube Delta: risks and responses. *Geo-eco-marina*, 4, p. 19 – 29.

Panin N., Jipa D., 2002 – Danube River Sediment Input and its interaction with the North-western Black Sea. *Estuarine, Coastal and Shelf Science*, 54, p. 551 – 562.

Panin N., 2003 - The Danube Delta. Geomorphology and Holocene Evolution: a Synthesis / Le delta du Danube. Géomorphologie et évolution holocène: une synthèse. In: *Géomorphologie: relief, processus, environnement*, 9 (4), Paris, 247 – 262.

Roelvink J.A., 2006. Coastal morphodynamic evolution techniques. *Coastal Engineering*, 53(2-3): 277 - 287.

Roelvink J.A., Reniers A.J.H.M., Dongeren A.R.V., van Thiel de Vries J.S.M., McCall R., Lescinski J., 2009. Modelling storm impacts on beaches, dunes and barrier islands. *Coastal Engineering*, 56.

Rusu, E., 2009. Wave energy assessments in the Black Sea, *J. Mar. Sci. Technol.*, 14, 359–372, doi:10.1007/s00773-009-0053-6, 2009.

Rusu, E., 2010. Modelling of wave-current interactions at the mouths of the Danube, *J. Mar. Sci.* Technol., 15, 143–159, doi:10.1007/s00773009-0078-x, 2010.

Sánchez-Arcilla A., García-Leon M., Gràcia, V., 2014. Hydro-morphodynamic modelling in Mediterranean storms - errors and uncertainties under sharp gradients. *Nat. Hazards Earth Syst. Sci.*, 14: 2993-3004.

Sánchez-Arcilla A., García-León M., Gràcia V., Devoy R., Stănică, A., Gault, J., 2016. Managing coastal environments under climate change: Pathways to adaptation. *Science of The Total Environment*, http://dx.doi.org/10.1016/j.scitotenv.2016.01.124

Sierra, J.P., Casanovas, I., Mosso, C., Mestres, M. and Sánchez-Arcilla, A., 2016. Vulnerability of Catalan (NW Mediterranean) ports to wave overtopping due to different scenarios of sea level rise. *Regional Environmental Change*, 16(5): 1457-1468.

Stănică A., Dan S., Ungureanu G., 2007 – Coastal changes at the Sulina mouth of the Danube River as a result of human activities. *Marine Pollution Bulletin*, 55, p. 555 – 563.

Stănică A., Dan S., Jiménez J.A., Ungureanu G.V. 2011 – Dealing with erosion along the Danube Delta coast. The CONSCIENCE experience

towards a sustainable coastline management. *Ocean & Coastal Management*, 54, 898 – 906.

Stănică A., Panin N., 2009 – Present evolution and future predictions for the deltaic coastal zone between the Sulina and Sf. Gheorghe Danube river mouths (Romania). *Geomorphology*, 107, 41 – 46.

Stockdon H.F., Holman R.A., Howd P.A., Sallenger, A.H., 2006 - Empirical parameterization of setup, swash, and runup. *Coastal Engineering*, 53, p. 573-588.

Tătui F., Vespremeanu-Stroe A., Ruessink G.B., 2016 - Alongshore variability of cross-shore bar behavior on a nontidal beach. *Earth Surf. Process. Landforms*, Wiley Online Library, DOI: 10.1002/esp.3974.

Ungureanu G., Stănică A., 2000 – Impact of human activities on the evolution of the Romanian Black Sea beaches. *Lakes & Reservoirs: Research and Management*, 5, p. 111 – 115.

Valchev N.N., Trifonova E.V., Andreeva N.K., 2012. Past and recent trends in the Western Black Sea storminess. *Natural Hazards and Earth System Science*, 12, 961-977.

Valentini, N., Saponieri, A., & Damiani, L. (2017). A new video monitoring system in support of Coastal Zone Management at Apulia Region, Italy. *J. Ocean & Coastal Management*, 142, 122-135.

van Geer P.F.C., Boers M., 2012 - Assessing dune erosion: 1D or 2DH? The Noorderstrand case study. *Jubilee Conference Proceedings, NCK-Days 2012*, 229-233. DOI: 10.3990/2.203

Vespremeanu-Stroe A., Constantinescu Ş., Tatui F., Giosan L., 2007 – Multi-decadal Evolution and North Atlantic Oscillation Influences on the Dynamics of the Danube Delta shoreline. *Journal of Coastal Research*, SI 50 (Proceedings of the 9th International Coastal Symposium), p. 157 – 162.

Vespremeanu-Stroe A, Preoteasa L. 2007. Beach–dune interactions on the dry–temperate Danube Delta coast. *Geomorphology* 86: 267–282.

Yankovsky A.E., Lemeshko E. M., Ilyin Y. P., 2004 – The influence of shelf-break forcing on the alongshelf penetration of the Danube buoyant water, Black Sea. *Continental Shelf Research* 24, p. 1083 – 1098.